EUROPEAN ORGANIZATION FOR NUCLEAR REASEARCH

KHR/afm CERN/PS-BR/83-28

AN APPROACH TO THE DESIGN OF SPACE-CHARGE LIMITED HIGH INTENSITY SYNCHROTRONS

K.H. Reich, K. Schindl, H. Schönauer
CERN, Geneva, Switzerland

(Paper to be presented at the XII th International Conference on High Energy Accelerators, Fermi National Accelerator Laboratory, Batavia, Ill., 11-16 August 1983).

Geneva, Switzerland
June 1983

AN APPROACH TO THE DESIGN OF SPACE-CHARGE LIMITED HIGH INTENSITY SYNCHROTRONS

K.H. Reich, K. Schindl, H. Schönauer
CERN, CH-1211 Geneva 23, Switzerland

Summary and Introduction

A design procedure for storage rings has been reported previously[1]. The approach proposed here concerns mainly synchrotrons which accelerate intense beams of protons or heavier ions; it could also be useful for the design of compressor or stretcher rings or similar facilities. The approach is based on experience gained in the involvement with half a dozen machines and in the design and development of the CPS Booster, which by now accelerates in one ring (vacuum chamber apertures 132 × 63 mm) 8 × 10^{12} ppp with 50 MeV injection.

The approach is presented as a commented (looped) flow chart (Fig. 1). Key limitations are: space-charge induced tune shifts, longitudinal coasting beam instabilities, and beam-loss induced radioactivity. Other items dealt with include the determination of the mean machine radius, RF parameters, beam emittances and energy spread required for stability, vacuum pressure, the length and number of long straight sections (lss), and a lattice yielding appropriate working room in the Q_H - Q_V diagram and transition energy. Relevant relations, graphs and empirical values for some critical parameters are given.

Recently half a dozen space-charge limited high-intensity AG rings have come under discussion for kaon, muon, neutron, neutrino, heavy-ion, etc. "factories", accelerating or compressing up to ~10^{16} pps. Five operational such accelerators have been designed in the last fifteen years[2-6]. Changes of emphasis at the design stage due to very high intensity are pointed out.

The information presented falls into three categories: (i) accelerator physics items of "permanent" nature, (ii) typical or limiting design values geared to machines with a mean radius of up to about 100 m and $B\rho$ up to 100 Tm, which could evolve further with technological progress, and (iii) suggestions based on personal judgement. MKS units are used throughout unless stated otherwise. The information provided (including key references), together with formula collections[7,8] and a pocket calculator, should allow one to arrive at a first basic parameter list not too much different from the final. The design proper would follow.

Mean Machine Radius $\bar{R}$ (= $C/2\pi$)

If $\bar{R}$ is not imposed, one starts from the bending radius:

$$\rho = p_{(eV/c)} / [qcB_{max}] , \qquad (1)$$

where p = max. particle momentum, c = velocity of light, B = magnetic induction in the bending magnets (on orbit), and q = number of electrical charges per particle. B < 1.1 T is usual for fast-cycling synchrotrons, < 1.3 T for slowly-cycling gradient magnets, and up to 1.6 T or even 2 T for flat field magnets. Conservative values are recommended to preserve field quality. Figure 2 gives R/ρ values[9] for (a) tight, and (b) conservative packing, recommended for long life component rating, avoidance of significant overlapping of magnetic end fields (stopbands), and space for local shielding and remote handling. Costs, notably for the RF accelerating and vacuum systems, and the machine enclosure, increase from a) to b).

Tunes, Amplitude Functions β, Periods N. To start the iteration, approximate values of the betatron tunes Q can be taken from Fig. 2. Further, one assumes $\bar{\beta} = \bar{R}/Q$, $\hat{\beta} \approx 3\bar{\beta}$, N ≈ 4Q and $\hat{D}(\approx \bar{R}Q^{-2}) \approx 1.2$ m.

Beam Injection

In case the injector pulse length is T_{inj} > (3 to 5) × T_{rev} (= revolution period), almost lossless (a few percent) injection is only feasible by charge-exchange, where e.g. H^- ions are stripped to protons in a thin foil[10]. For classical betatron stacking, the achievable injection efficiency can be estimated roughly (neglecting the width D $\Delta p/p$ with D = dispersion):

$$\eta_{inj} \approx 0.9 \left\{ 1 - \exp\left[- \left(A^{1/2} - (n_t/\beta_{Hsept})^{1/2} t_{seff} \right)^2 / (n_t \varepsilon_{0H}) \right] \right\} \qquad (2)$$

where A_H = horizontal acceptance, $n_t = T_{inj}/T_{rev}$, T_{seff} = effective septum thickness, and the emittance ε_{0H} contains 63% of the injector beam. For low injector currents and long pulses with small $\Delta p/p$ stacking in longitudinal phase space is an alternative[5].

RF Parameters

RF Voltage

Acceleration. As in all synchrotrons with negligible synchrotron radiation, the energy gain per turn is given by:

$$\hat{V}_{RF} \cdot \sin\phi_s = C\rho\dot{B} \qquad (3)$$

where $\hat{V}_{RF}$ is the peak RF voltage per turn, ϕ_s is counted from the zero crossing, and $\dot{B}$ = dB/dt.

Longitudinal Acceptance. Below transition energy the space-charge field reduces the zero-particle longitudinal acceptance (least for h = 1), and the RF voltage must be increased accordingly[7,11]. An acceptance margin of, say, 30% is recommended for low loss trapping.

Harmonic Number

Choice of the harmonic number (h = f_{acc}/f_{rev}): h = 1 leads to (i) the lowest peak voltage, because the voltage required for providing longitudinal acceptance increases with h; (ii) the absence of coupled bunch instabilities (still true for h = 2); (iii) the longest rise time and hence to least stress (and cost) for any fast ejection kicker magnet; but also to (iv) only one bunch, not dividable "losslessly" among several users; (v) the smallest bunching factor B_f (<1), because, for fixed $V_{RF}.\sin\phi_s$, the lowest V_{RF} leads to the highest $\sin\phi_s$ and hence the shortest bunch (in RF radians); (vi) the need for a more complex phase control system if more than two cavities (assuming N even) are required. While in general for machines of the size considered, the optimum (including engineering criteria) is anywhere from, say, h = 4 to 20, h = 1 or 2 clearly has advantages in the present context.

To bring the peak line density further down towards the value of the mean density, a higher harmonic RF system can be added[12]. Within certain limits[13] this may also provide extra Landau damping.

Beam Loading Compensation

At the high intensities under discussion (RF Fourier component of beam current > RF cavity drive current) such a compensation is likely to be needed, particularly during adiabatic trapping and any other "gymnastics" with reduced RF voltage. Servo-loop techniques[13-15] are more cost effective than high power solutions.

Beam Emittances (Space-Charge Detuning)

During injection and initial acceleration beam emittances $\epsilon_{H,V}$ (in π radm) have to be controlled in such a way that the space-charge detuning ΔQ_{sc} does not drive the beam into stopbands causing unacceptable beam loss (see betatron resonances below). The largest ΔQ_{sc} is experienced by particles with vanishing betatron amplitudes at the bunch centre. For the usual beams (width > height because of magnet field cost) the largest (negative) detuning is given by[7]:

$$\Delta Q_{scV} = \frac{r_p \, N_I (q^2/A) F_V G_V \bar{H}_V}{\pi \, (\epsilon_V \beta\gamma) \, \beta\gamma^2 B_f} \qquad (4)$$

where r_p = classical proton radius, N_I = number of ions circulating, A = ion mass in multiples of proton mass m_p, β and γ = usual relativistic factors, and F_V, G_V, $\bar{H}_V$ = form factors discussed below.

Bunching Factor. B_f (= average/peak line density) decreases with increasing stable angle ϕ_s (in rad) and is

$$B_f \approx (2/\pi)\left[1 - (\phi_s + 3.6\sqrt{\phi_s})/2\pi\right] \qquad (5)$$

for a full bucket (and 10% less in practice); $\gamma < \gamma_{tr}$. The term $\beta\gamma^2 B_f$ in (4) can well reach its minimum some time after acceleration starts, particularly in fast-cycling synchrotrons.

ΔQ_{sc} and Form Factors. The maximum admissible value for ΔQ_{sc} depends on the stopband respectively beam loss situation, and the ΔQ margin to be reserved notably for chromaticity and amplitude dependent Q-shifts. ΔQ_{scV} = 0.25 is a starting value. F_V contains the Laslett image coefficients[7,8]; for $\gamma \approx 1$: $F_{H,V} \approx 1$.

Table 1. G for Various Distributions in Physical Space.

Distribution	$G_{H,V}$	% beam in $\epsilon_{H,V}$
Uniform	1	100%
Parabolic density	2	100%
" "	1.56	95%
Gaussian	1.56	98%
PSB, best measured[16]	G_H = 1.37	95%
(Proton injection)	G_V = 1.23	95%

G_V (Table 1) describes the transverse density distribution. A well designed H^- charge-exchange injection should yield $G_{H,V}$ = 1.2 to 1.3; classical multiturn injection results in G_V = 1.5 to 2. H_V takes into account the beam aspect ratio width/height, and its variation with the amplitude function $\beta_{H,V}(s)$:

$$H_V = \left[1 + \sqrt{(\epsilon_H \beta_H + D \, \Delta p/p)/(\epsilon_V \beta_V)}\right]^{-1} . \qquad (6)$$

in smooth approximation, for $\Delta p/p$ = 0, and averaging over a (super)period[16]:

$$\bar{H}_V \approx (1 + \sqrt{\epsilon_H/\epsilon_V} \, \sqrt{Q_V/Q_H})^{-1} . \qquad (6a)$$

Using $\bar{H}_H + \bar{H}_V = 1$,

$$\Delta Q_{scV}/\Delta Q_{scH} = \sqrt{\epsilon_H/\epsilon_V}/\sqrt{Q_V/Q_H} . \qquad (7)$$

Thus, with ΔQ_{scV} more critical ($\epsilon_V < \epsilon_H$), raising Q_V/Q_H helps. For ΔQ_{scV} = 0.25 to 0.5, $\Delta Q_V/\Delta Q_H$ = 1.5 to 2 is recommended for avoiding the stopband intersections on the diagonal $Q_H - Q_V$ = integer. (7) thus yields ϵ_H/ϵ_V, and with (4) ϵ_H. In a machine with a sizeable relative beam width due to momentum spread, ϵ_H may be reduced correspondingly.

Longitudinal Stability[8,17,18] (Momentum Spread)

Only the coasting beam is dealt with as long bunches can be stabilised by an electronic feedback system[19]. To estimate the growth during the critical phase (prior to capture) one computes the impedance (at $\omega = n\omega_{rev}$) due to the space-charge and various resonators:

$$\frac{Z_\parallel(n)}{n} = -j \frac{Z_0 \, g}{2\beta\gamma^2} + \Sigma \frac{1}{n} \frac{R_s}{1 + jQ\left[(\omega/\omega_r) - (\omega_r/\omega)\right]} \qquad (8)$$

with $Z_0 = 377\Omega$ and $g = 1 + 2\ln(b/a)$, (b = chamber radius, a = beam radius). The resonators comprise (i) RF cavities (tunable) with $Q \approx 100$, $R_s \approx$ a few kΩ and $\omega_r \approx h\omega_{rev}$, (ii) a broad-band resonator with $\omega_r \approx c/b$, Q = 1 and $R_s = (\bar{R}/\beta b)\left|[Z_\parallel(n)/n]\right|_{\omega\to 0} \approx (\bar{R}/\beta b) \times 10$ to 15 Ω for a well engineered machine, or possibly lower with extra effort[6]; (iii) known or likely parasitic resonators like a fast kicker magnet[20] with $Q \approx 1$ to 2, $R_s \approx$ tens of Ω and $\omega_r \approx$ 10 MHz. As the first term is dominant at lower energies, application of the Keil-Schnell-Boussard criterion:

$$\left|\frac{Z_\parallel(n)}{n}\right| < \frac{(m_p c^2/e_{(v)})\beta^2\gamma|\eta|}{I_I \, q/A} \left(\frac{\delta p}{p}\right)^2_{FWHH} \qquad (9)$$

[with $\eta = \gamma_{tr}^{-2} - \gamma^{-2}$ and I_I = the (local) ion particle current] may yield values too pessimistic by a factor up to three depending on the distribution. The growth rate (neglecting Landau damping): (10)

$$\frac{1}{\tau(n)} < n\omega_{rev} \left[\frac{|\eta| I_I \, q/A}{8\pi \, \beta^2\gamma(m_p c^2/e)} \, \frac{1}{\mathrm{Im}[Z_\parallel(n)/n]}\right]^{1/2} \mathrm{Re}\left[\frac{Z_\parallel(n)}{n}\right]$$

should be checked around n = h (effect of RF cavity) and $n = n_c = \gamma\bar{R}/b$ (microwave instability). If the beam coasts for more than 3 to 4 e-folding times, the momentum spread will increase at least until the stability criterion (9) is fulfilled. Acceptance (physical and in terms of RF voltage) must be planned accordingly.

Transverse Stability[8,17,18]

For a round beam pipe (space-charge + resistive wall) and resonators the transverse coupling impedance is:

$$Z_\perp(\omega) = -jRZ_0\beta^{-2}\gamma^{-2}(a^{-2} - b^{-2}) + (1 + j)RZ_0 \, b^{-3}\delta + Z_{\perp\,kickers}^{20} + Z_{\perp\,cavities} \qquad (11)$$

$$\text{where } \delta = \begin{cases} \delta(\omega) = \sqrt{2\rho/(\mu_0\omega_r\omega)} & \text{for } \delta(\omega) < t_w \\ t_w & \text{for } \delta(\omega) > t_w \end{cases}$$

with t_w the wall thickness and $\rho \approx 10^6$ Ωm for stainless steel.

Typical values for a PSB type machine are $Z_\perp \sim 10^5 + j\,10^8$ Ω/m at 1 MHz for the vacuum chamber, and $\mathrm{Re}(Z_\perp) \sim$ 40 kΩ/m around 10 MHz per metre kicker length. The transverse stability criterion is too pessimistic in this context as -in contrast to high energy machines- additional Landau damping arises from amplitude dependent space-charge detuning.

Stabilisation. (i) integer < Q < half-integer is recommended as otherwise the resistive wall impedance may become uncomfortably high for the smallest frequency $(n - Q)\,\omega_{rev}$ (n > Q); (ii) conventional Landau damping by octupoles enlarges stopbands and should be avoided; (iii) the favoured remedy (least unwanted side-effects and cost) is an electronic damper[21], generating a transverse impedance[22] offsetting the driving one $-\mathrm{Re}(Z_\perp)_{damper} > \mathrm{Re}(Z_\perp)_{machine}$, up to $\omega/2\pi \approx$ 50 MHz (coasting beam) or $\omega \approx 4/(2\pi \times$ bunch duration) (bunched beam).

Limitations Due to Machine Irradiation

Exposure to induced radioactivity accounts for almost all of the doses received by accelerator staff.

A simple approach to estimate the average properties of the radioactive isotopes produced in high energy particle interactions can be used to predict the induced radioactivity with sufficient accuracy, provided many different isotopes are formed and the distribution of their half-lives is not too different from a natural one. Using these approximations, it is estimated that a thick target (beam dump) of iron or copper irradiated with a beam of ΔN_{IS} protons/s of an energy greater than about 200 MeV (isotope production cross-section ≈ const.) will produce at 40 cm distance a dose-rate[23]:

$$D_{(rem/h)} \approx 2.3 \times 10^{-12}\ \Delta N_{IS}\ \log[(T+t)/t] \qquad (12)$$

with T the irradiation time, and t the cooldown time. Thus, for T = 30d, t = 1d and $\Delta N_{IS} = 3 \times 10^{11}$ p/s, D ≈ 1 rem/h. For heavier ions, the constant in (12) has to be scaled by the ratio of the total inelastic cross-sections[24] (for the target material). In practical situations the beam may first hit an accelerator component which does not represent a thick target. The dose rate calculated will then be smeared out over a certain distance rather than be concentrated. Dose-rates from lighter materials such as graphite or limestone, are up to two orders of magnitude lower. However, (12) will give a value (at 40 cm) which has to be anticipated when discussing controlled loss in beam catchers, for instance at (injection and) ejection, and "general" loss (from RF trapping, betatron resonances, etc.). Judging from present experience, it seems very hard to keep the latter below a few percent.Hence accelerating 10^{15} p/s probably means facing up to dose-rates of the order of 100 rem/h unless exceptional measures are taken (see below). At proton energies below about 200 MeV induced activity dose-rates are much reduced and will be more than an order of magnitude less at 50 MeV. Hence correspondingly higher injection, capture and resonance losses can be stood. Hands-on maintenance is limited to D < a few rem/h.

The damage to accelerator components resulting from irradiation depends on the type of material, the type of radiation, temperature, humidity, etc. Again, for a very rough first check, the yearly dose to a "thick target" can be estimated from:

$$D_{IR(rad/y)} \approx 3 \times 10^{-10}\ \Delta N_{Iy}\ , \qquad (13)$$

where ΔN_{Iy} = number of irradiating protons per year.

Control of Beam Loss and its Effects

Main points are (i) studying and limiting beam loss to far below what would be acceptable by the beam users (beam injection, RF capture, betatron resonances, instabilities, ejection, etc.); (ii) concentrating beam loss in beam lines, at injection, when dumping internally, at ejection, etc. in tailor-made beam dumps[6] (made from low-radioactivity material like graphite or shielded e.g. by limestone; (iii) avoiding potential interventions in radioactive areas by housing whenever possible equipment outside the machine enclosure and increasing the lifetime of components housed inside (conservative ratings[25], use of high-grade radiation resistant materials, remedial actions against specific beam loss effects like local overheating, increase of the ozon content of the air with the consequent corrosion effects, degradation of demineralised cooling water with the resulting blockage of thin cooling passages, etc.); (iv) reduction of time for actual interventions through the use of rapidly exchangeable modular "plug in" type components; (v) provision of remote handling of potentially all, but at least of critical components such as septum magnets (and their enclosure), beam dumps, etc. The radiation shielding is based on the well established techniques developed around accelerators and storage rings. At the intensities under consideration, air conditioning and water cooling have to be closed-circuit designs (for keeping the outside radioactivity at legally acceptable levels). Most of these questions have recently been studied for a 3×10^{16} pps 1100 MeV proton linac[26].

Betatron Resonances

A particle experiences unlimited betatron amplitude growth if its tunes Q_H, Q_V satisfy:

$$|mQ_H + nQ_V - p| < \Delta e/2, \qquad m,\ n,\ p \text{ integers} \qquad (14)$$

where m + n is the order of the resonance and $\Delta e/(m+n)$ the total stopband width in the Q_H - Q_V diagram. Stopband considerations determine (i) ΔQ_{SC}, (ii) the requirements on magnet field quality[27], and (iii) the need for harmonic correcting multipoles. Before going into a full analysis[17,28], a rough consideration of the one-dimensional resonances serves to assess the magnitude of the problem on hand.

<u>Stopband Width and Amplitude Growth.</u> Limiting oneself to the vertical plane (m = 0), the pth Fourier component of a magnet imperfection $\partial^{(n-1)}B_{z,x}/\partial x^{(n-1)}$ excites a stopband of width:

$$\Delta e \approx \frac{\bar{R}}{\pi B\rho} \left\{ \begin{array}{l} \int_0^{2\pi} \beta_z \frac{\partial B_z}{\partial x} \\ \frac{3}{8}\sqrt{\varepsilon_V} \int_0^{2\pi} \beta_z^{3/2} \frac{\partial^2 B_x}{\partial x^2} \\ \frac{1}{12}\varepsilon_V \int_0^{2\pi} \beta_z^2 \frac{\partial^3 B_z}{\partial x^3} \end{array} \right\} \cos p\theta\, d\theta, \left\{ \begin{array}{l} n = 2 \text{ (quadrupole)} \\ n = 3 \text{ (skew sextupole)} \\ n = 4 \text{ (octupole)} \end{array} \right. \qquad (15)$$

where β_z is the amplitude function at the driving elements. Of particular concern here is the ε-dependence of Δe for non-linear resonances.

<u>Growth Rate for Coasting Beam.</u> A very rough estimate of the initial loss rate, without considering amplitude dependent space-charge detuning, can be made assuming that (i) the aperture is completely filled, (ii) at the beam edge the number of particles N contained up to amplitude r is proportional to r, and (iii) the fraction of the particles locked on resonance is $(\Delta e/n)/\Delta Q_{SC}$:

$$\frac{1}{N_I}\frac{dN_I}{dt} \approx -\frac{\pi}{T_{rev}}\frac{1}{\Delta Q_{SC}}\left(\frac{\Delta e}{n}\right)^2 \ . \qquad (16)$$

<u>Growth Rate for Bunched Beam.</u> The particle is repetitively swept over $nQ_V - p = 0$, twice during one synchrotron oscillation period. With the same assumption as in the coasting beam case, and supposing that all particles are swept over the stopband considered (but do not lock on), one can estimate the approximate beam loss during time Δt:

$$\frac{1}{N_I}\frac{\Delta N_I}{\Delta t} \approx -\frac{\Delta e}{n}\sqrt{\frac{\beta c}{2\bar{R}n\ \Delta Q_{SC}\Delta t}} \qquad (17)$$

<u>Data.</u> In Table 2 computed loss rates at ~50 MeV for the PS Booster (4 rings, 16 magnet periods, imperfections in bending magnets $|\Delta B/B| < 2 \times 10^{-4}$) are shown, using Δe values computed from magnet measurements or measured in beam experiments[29].

<u>Assessment.</u> (i) Assume a maximum field error $|\Delta B/B|$ at the edge of the chamber aperture at injection field (where ΔQ_{SC} is large) and compute the relevant multipole coefficients; (ii) derive rms values of the width of (non-systematic) stopbands (produced by k types of elements each having N_k elements of length L_k) from (15) where the integral is replaced by the sum:

$$\left\{\sum_k (N_k/2)\left[\beta_{zk}^{n/2}(L_k/\bar{R})\,\partial^{(n-1)}B_{z,x}/\partial x^{(n-1)}\right]^2\right\}^{1/2}; \qquad (15a)$$

Table 2 - Stopband widths and Loss Rates in the PS Booster

n	Stopband (syst.)	Δe ranging from	to (* measured)	Loss rate $1/N_I\ \Delta N_I/\Delta T$ if aperture filled: Coasting beam initial loss rate (ms^{-1})		Bunched beam average loss rate within 1 ms (ms^{-1})		1 s (s^{-1})
2	$2Q_v = 11$	0.004*	0.007*	0.030	0.092	0.126	0.221	-
3	$3Q_v = 16$	0.002*	0.016*	0.0033	0.214	0.034	0.275	-
	$3Q_v = 14$	0.0008		0.00053		0.0068		0.440
4	$4Q_v = 21$	0.0001		4.7×10^{-6}		0.0011		0.035

(iii) compute loss rates for coasting and bunched beams (16, 17); (iv) if losses are too fast, consider improved magnet quality or plan for stopband compensation by appropriate multipoles[17, 27-29] from the start. PSB stopbands were narrowed by a factor 10 to 30 (n = 2,3).

Vacuum Pressure[8]

Avoiding significant emittance blow-up due to collision with the residual gas is usually no problem with modern all-metal and ceramic vacuum systems achieving with some care 10^{-8} torr or better. Depending on energy and charge state, ions may well require a lower pressure to avoid charge exchange[30].

Stability Against Electron-Proton (Ion) Oscillations. A low vacuum pressure could be required to ensure that the relative neutralisation stays below a threshold value η_{thr} . Otherwise electrons created by ionisation of the residual gas and trapped in the potential well of a coasting ion beam (and sometimes in the well of long bunches) give rise to rapidly growing transverse oscillations[31]. For large ΔQ_{sc} one has with (6):

$$\eta_{thr} \approx (2.8\ B_f \gamma^2)^{-1} (H_{Vmax} - H_{Vmin})/\bar{H}_V \qquad (18)$$

Measurements[32] suggest a neutralisation rate:

$$\dot{\eta} = 6 \times 10^7\ q^2\ P_{(Torr)} [10.1 + \ln\beta^2\gamma^2 - \beta^2]/\beta \ . \qquad (19)$$

In general, highest η_{thr} values occur at injection. For a linear current build-up one has $\eta \approx 0.5\ \dot{\eta}\ T_{inj}$. The pressure (19) must be such that $\eta < \eta_{thr}$ (18).

Machine Lattice

Contrary to the other items, lattice selection and design cannot be solved approximately by a few (rough) calculations. Even a short lens approach[17] would exceed the scope of this paper. However, one has here at least a check list of the items to be considered (except correction elements) and a reminder of certain consequences of parameter variations. This should help to fix the initial configuration for the iterative computer-aided optimisation[1, 33].

Superperiods or Not ?

Providing a total of two lss for injection, ejection and possibly RF accelerating cavities, i.e. S = 2, would probably lead to the shortest circumference, but also to systematic (structural) stopbands. The decision about superperiods should thus be based on a Q_H -Q_V diagram showing all such stopbands p = kS up to order 4 or even 5, and a loss assessment. For a number of periods N larger than, say, 12, S = N/2 could possibly be an acceptable compromise (the larger S, the fewer such stopbands) which would notably still allow equidistant distribution of the RF cavities. A lattice without superperiods may, however, be preferred for simplicity and possibly minimum magnet energy stored, and for easier B tracking and smaller likelihood of standing wave modes (leading to unequal magnet excitation) in the case of fast-cycling machines.

Minimum Length of Long Straight Section.

With a fixed machine radius and in the absence of superperiods one upper limit for N is reached when the lss becomes too short for housing the most critical piece of equipment.

Beam Ejection. If D_b is the beam displacement required to eject the beam from a straight section of length L_{lss} by means of a septum magnet with an induction B_s occupying the upstream fraction f L_{lss} one has (for zero septum entrance angle) (Fig. 3):

$$L_{lss} \approx \sqrt{[D_b/(B_s B\rho)]/(f - f^2/2)} \ . \qquad (20)$$

D_b/B_s = 0.05 m/T applies to ejection through a D gradient magnet or past a "septum" bending magnet; 0.2 to 0.3 m/T are normal. Larger L_{lss} values may be required to eject (large emittance) beams with kicker and septum magnets on either side of a D lens (no aperture increase elsewhere). f < 0.7 is recommended.

RF Accelerating Cavity. Modern tunable ferrite-loaded cavities are often designed as double-gap units about 2.5 m long (delivering approx. 20 kV in the MHz range, or 50 kV in the tens of MHz range and $f_{final}/f_{initial}$ < 2). Below about 2 GeV kinetic proton energy the RF cavity determines the straight section length, and beam ejection above (assuming that injection takes less space).

Number of Long Straight Sections and Periods N.

Space requirements for injection (1), acceleration (say, 1 to 16), ejection (1 to 3), beam observation (1) and spares (1 to 2) give about 6 to 22 lss (for one ejected beam). N = 6 would lead to excessive apertures for the large emittances and sizeable momentum spreads considered, and probably to an inconvenient γ_{tr} . Inscreasing N (and Q) for fixed machine radius and vacuum chamber dimensions increases, (i) the vertical and even more the horizontal acceptances, (ii) the range of betatron tuning, but also, (iii) the number and strength of quadrupoles (in case of a separate function magnet), (iv) the number of correction elements and beam position monitors, (v) the space taken up by the coil ends and the power dissipated in them, and (vi) the number of "unoccupied" lss. It decreases, (i) the straight section length available for injection and ejection, (ii) the length available for quadrupoles (and correction elements). The fraction of the circumference taken up by the bending magnet yokes, RF cavities, pump manifolds and general beam diagnostics is left unchanged.

Thus, the choice of N could be guided by a cost optimisation: purchasing and operating cost for a lesser number of wider aperture elements and their power supplies vs a higher number of smaller aperture elements.

More on Q Values

Phase Advance of Betatron Oscillations/period

In case of a FODO lattice, $\mu \approx 75°$ leads to a (broad) minimum of the maximum amplitude function (≈ 1.7 L_{period} [17]). For fast beam ejection the deflection needed by the kicker magnet is:

$$\Theta_k = \frac{w_s[=f(\beta_{septum})] + t_s + \Delta}{\sqrt{\beta_{kicker} \cdot \beta_{septum}} \cdot \sin\mu_{kicker \to septum}} \qquad (21)$$

where w_s = beam width at the septum magnet, t_s = septum thickness, and Δ = safety margin. Apart from a large β_{kicker} , μ = (2k + 1) 90° between kicker and septum magnets is hence most favourable.

Table 3 - Some Types of Lattice Periods

Period	Advantages	Drawbacks
FODO	- Lowest gradients in lenses*). - Two lenses per cell (only). - Chromaticity and stopband corrections with sextupoles well decoupled in H and V planes.	- Strong variation of amplitude functions in lss (inefficient use of aperture of elements in lss, unless divided into sections with different apertures).
OFDO	- Longer lss than in FODO case - $\beta_{H,V}$ variations over same distance in lss less marked than for FODO. - Two lenses*) per cell. - Chromaticity and stopband corrections fairly decoupled.	- Gradients higher than for FODO.
Triplet (OFDFO or ODFDO)	- Both β_H and β_V small in lss (smallest aperture for magnets, RF cavity, etc.) - If $\epsilon_V/\epsilon_H = \beta_H/\beta_V$ in central lens, efficient use of single lens aperture.	- One extra lens*) compared to FODO. - Chromaticity and stopband corrections not very effective (coupled).
FOFDOD resp. FOOFDOD or FOFDOOD	- β_H/β_V change least in lss (efficient use of single aperture). - Choice of appropriate $\beta_{H,V}$ values for injec- and ejection. - Chromaticity and stopband corrections well decoupled.	- Two extra lenses*) compared to FODO. - Higher gradients than in FODO.

*) Gradient magnets in case of combined function magnets, in which case "extra lenses" will not increase the total magnet yoke length.

Third order resonance excitation by sextupoles (of the same family) used for chromaticity correction is avoided if they are arranged in pairs with an odd number of half betatron wavelengths between them. Apart from N = even, this favours $\mu = 90^\circ$ or 60°.

Q-Splitting. $Q_V - Q_H = 1$ (or even 2) will raise the space-charge limit (7), avoid the stronger zeroeth harmonic non-linear coupling resonances, and is recommended. The price to be paid may be larger β values at least in one plane, and a greater difficulty in finding a region free of systematic stopbands. In case high γ_{tr} is an overriding constraint, $Q_H > Q_V$.

Combined or Separate Function Magnet ?

Combined function magnets are a cost-effective way to achieve high N focusing structures even using quadruplets, and may well be the choice for a fast-cycling synchrotron where losses due to stopbands are less critical. A separate function magnet would probably be the choice for a slow-cycling or dc machine since (i) an experimentally optimized (dynamic) $Q_H - Q_V$ working area could be implemented more easily, and (ii) stopbands are likely to be narrower. Also, it can be "recycled" more easily. A hybrid solution (gradient magnets plus lenses) may combine the best features of the two.

Type of Lattice Period

For a first orientation, the information given in Table 3 may be helpful. A (separate function) OFDO lattice could be a good compromise between the minimum FODO lattice and a more refined one. An OFDO lattice with an auxiliary short dc lens has also been proposed to take advantage of the increased machine acceptance at low energies[34].

Transition Energy

While up to 2×10^{13} protons per pulse are routinely accelerated through transition in the CERN PS due to the γ_{tr} jump[35], "lossless" crossing may become even more difficult at substantially higher intensities. Beam ejection becomes tricky or impractical around transition, thus there is an incentive to shift γ_{tr} to well above top energy. While the type of lattice chosen has some influence[34] (say, ±15%), basically $\gamma_{tr} \approx Q_H$; it can thus be raised by raising N and hence Q. If that is not enough, more sophisticated methods are available based either on extra lenses[35, 36] or on creating an azimuthal pattern of bending magnet positions or lens strengths[34].

* Recent rather than the original references are given.

Acknowledgements

We thank our colleagues for a number of discussions which have been useful for this paper, and Mrs. A. Molat-Berbiers for typing it.

References*)

1) E. Keil, Proc. IXth Int. Acc. Conf., Stanford, 1974, pp. 660-69
2) R. Billinge et al., IEEE NS-16, 1969, pp. 969-74.
3) K. Schindl et al., IEEE NS-28, 1981, pp. 2803-05.
4) Y. Arakita et al., IEEE NS-24, 1977, pp. 1544-56.
5) J.P. Aknin et al., IEEE NS-26, 1979, pp.3138-42.
6) G.H. Rees, IEEE NS-28, 1981, pp. 2125-27.
7) C. Bovet et al., CERN/MPS-SI/Int.DL/70-4, 1970.
8) G. Guignard, CERN 77-10 and references quoted, 1977
9) J.H.B. Madsen, P.H. Standley, Suppl. Proc. XIth Int. Acc. Conf., CERN, 1980.
10) C. Ankenbrandt et al., Proc. XIth Int. Acc. Conf., CERN, 1980, pp. 260-71.
11) A. Hofmann, F. Pedersen, IEEE NS-26, 1979, pp. 3526-28.
12) L.Z. Barabash et al., Proc. Charged Particle Acc. Conf., Moscow, 1968, Vol.II, pp. 123-27.
13) J.M. Baillod et al., IEEE NS-30, 1983.
14) F. Pedersen, IEEE NS-22, 1975, pp. 1906-09.
15) D. Boussard et al., IEEE NS-26, 1979, pp. 3569-70.
16) J.P. Delahaye et al., Proc. XIth Int. Acc. Conf., CERN, 1980, pp. 299-304.
17) Erice Acc. School, CERN 77-13 and Fermilab Acc. School, AIP Conf. Proc. N° 87, New York, 1982.
18) J.C. Laclare, Proc. Symp. HIF, GSI, Darmstadt, Germany, 1982, pp. 278-89.
19) B. Kriegbaum et al., IEEE NS-24, 1977, pp. 1695-97.
20) G. Nassibian, F. Sacherer, Nucl. Instr. Meth., Vol. 159, 1979, p. 21-27.

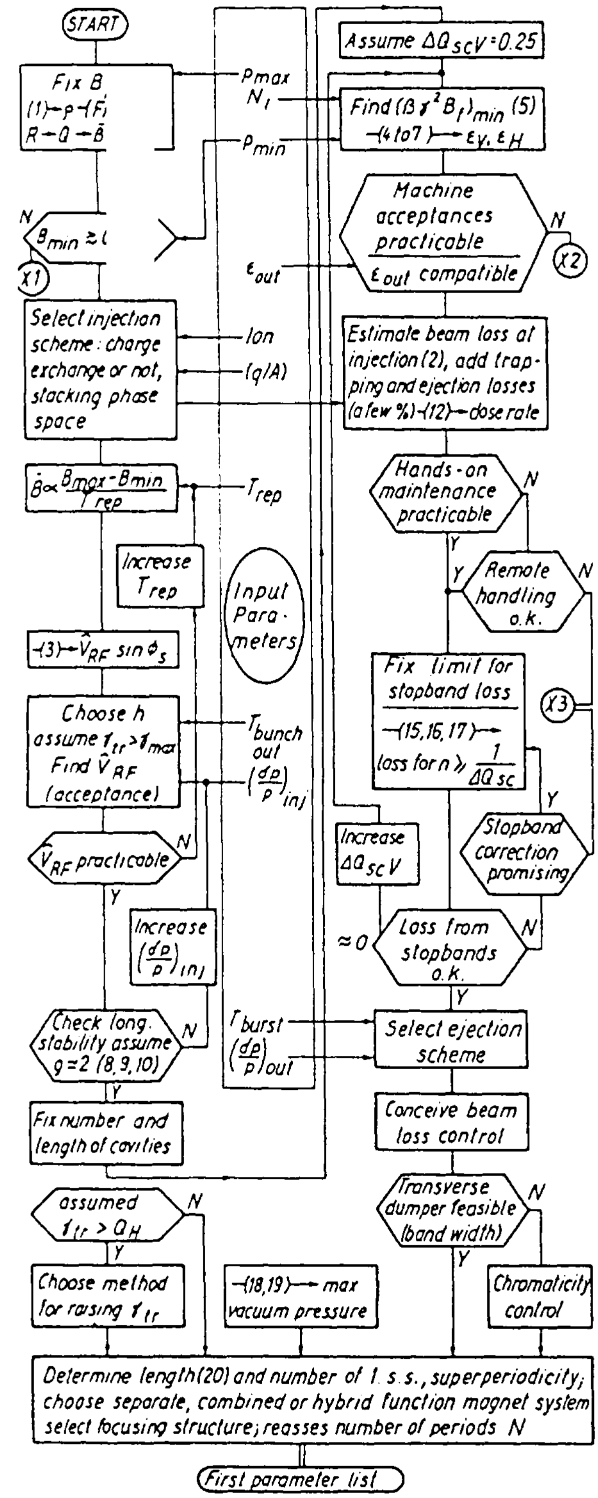

X Start again with modified input parameters :
X1 increase B_{max}, p_{inj}
X2 increase p_{inj}, number of rings; reduce N_l, T_{rep}
X3 reduce N_l

Fig. 1 - Proposed Approach. () refers to equ. in text.

21) C. Carter et al., IEEE NS28, 1981, pp. 2270-72.
22) F. Pedersen et al., IEEE NS-30, 1983.
23) A.H. Sullivan, Health Phys., Vol. 23, 1972, pp. 253-55.
24) S. Barshay et al., Phys. Rev. C, Vol. 11, 1975, p. 360-69.
25) G. Nassibian et al., IEEE NS-24, 1977, pp. 1551-53.
26) SNQ Studie, Teil III, Annex B, Band 5, KfK Karlsruhe, Germany, 1981.
27) C. Bovet et al., Proc. VIIIth Int.Acc. Conf., CERN, 1971, pp. 380-83.
28) G. Guignard, CERN 78-11 and references quoted, 1978
29) K. Schindl, IEEE NS-26, 1979, pp. 3562-64.
30) B. Franzke, IEEE NS-28, 1981, pp. 2116-18.
31) E. Keil, B. Zotter, CERN-ISR-TH/71-58, 1971.
32) W.H. De Luca, IEEE NS-16, 1969, pp. 813-22.
33) EPS Conf. on Comp. in Acc. Design, Berlin, 1983.
34) B. Franczak et al., IEEE NS-30, 1983.
35) W. Hardt, Proc. IXth Int. Acc, Conf., Stanford, 1974, pp. 434-38.
36) J.P. Delahaye, A. Krusche, IEEE NS-30, 1983.

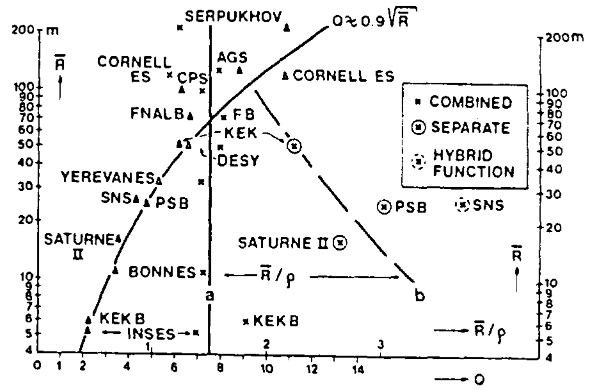

Fig. 2 - $\bar{R}$ vs $\bar{R}/\rho$ (×) and $\bar{R}$ vs Q (Δ)[9] for all AG synchrotrons in operation[9]. (ES = electron synchrotron).

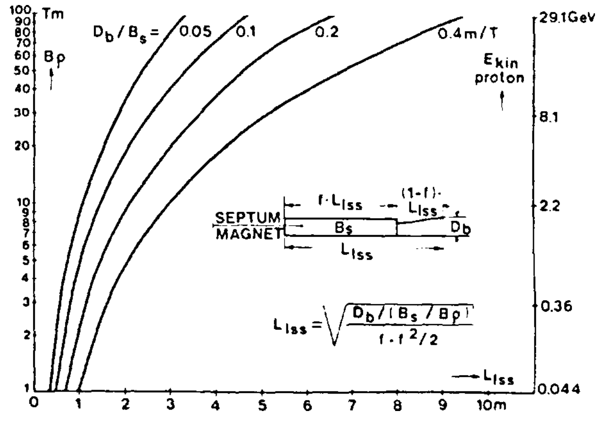

Fig. 3 - Magnetic rigidity Bρ (respectively kinetic proton energy) vs length of ejection straight section L_{lss} for f = 0.7.